Tunable refraction effects in two-dimensional photonic crystals utilizing liquid crystals

Hiroyuki Takeda and Katsumi Yoshino
Department of Electronic Engineering, Graduate School of Engineering, Osaka University, 2-1 Yamada-oka, Suita, Osaka 565-0871, Japan

(Received 9 August 2002; revised manuscript received 7 November 2002; published 9 May 2003)

Tunable refraction effects in two-dimensional photonic crystals utilizing liquid crystals are theoretically demonstrated. Due to liquid crystals with anisotropies, the incident light propagates in photonic crystals at refractive angles different from those in photonic crystals composed of isotropic materials. Moreover, refractive angles can be changed by rotating the directors of liquid crystals. Tunable refraction effects are also discussed for the light with two kinds of frequencies: one is a frequency at the edge of a band gap, and the other is a frequency a little far from the edge of a band gap.

DOI: 10.1103/PhysRevE.67.056607 PACS number(s): 42.70.Qs

I. INTRODUCTION

Recently, refractive-index regular structures have attracted much attention as photonic crystals from both fundamental and practical viewpoints, because novel concepts such as photonic band gaps have been predicted, and various new applications of the photonic crystals have been proposed [1–3]. In earlier work, two fundamentally new optical principles, namely, the localization of light [4–6] and the controllable inhibition of spontaneous emission of light [7–10] were considered to be the most important. In order to obtain photonic band gaps, we must use materials with high refractive indices such as Si, GaAs, and so on. In such materials, however, refractive indices cannot easily be changed by external factors such as temperature and electric fields.

On the other hand, properties of liquid crystals (LCs) can easily be changed by electric fields. For many applications, it is useful to realize tunabilities of photonic band structures through electro-optic effects. Therefore, tunable photonic crystals infiltrated with liquid crystals in which optical properties can be controlled by temperature and applied electric fields have been proposed [11–16]. Indeed, refractive indices of liquid crystals are low and therefore, photonic crystals infiltrated with liquid crystals have no photonic band gaps. However, such photonic crystals provide various applications even if they have no photonic band gaps.

For example, ultrarefractions and negative refractions have been reported recently [17,18]. They are obtained from high dispersion relations between frequencies and wave vectors regardless of the existence of photonic band gaps. Therefore, we can obtain ultrarefractions and negative refractions from photonic crystals composed of liquid crystals with low refractive indices.

In this paper, we demonstrate tunable refraction effects in two-dimensional photonic crystals utilizing liquid crystals. In conventional two-dimensional photonic crystals, two modes, namely, the transversal electric (TE) mode and the transversal magnetic (TM) mode exist. In photonic crystals composed of liquid crystals, generally, no such classifications of modes exist due to anisotropies of liquid crystals. Even in such photonic crystals, however, we can classify the TE and TM modes in the cases of directors of liquid crystals parallel and perpendicular to two-dimensional planes.

Therefore, we treat the case of directors of liquid crystals parallel to two-dimensional planes and the TE mode, because electric fields exist only in two-dimensional planes in the case of the TE mode, and are strongly affected by rotating directors of liquid crystals.

II. THEORY

Following the discussion of Busch and John [14], we start with the wave equation satisfied by the magnetic field for two-dimensional periodic structures in order to determine photonic band structures of two-dimensional photonic crystals utilizing liquid crystals.

$$\nabla\times\{\epsilon^{-1}(\mathbf{r})\nabla\times\mathbf{H}(\mathbf{r})\}=\frac{\omega^2}{c^2}\mathbf{H}(\mathbf{r}), \tag{1}$$

where $\nabla\cdot\mathbf{H}(\mathbf{r})=0$. The dielectric tensor $\epsilon(\mathbf{r})=\epsilon(\mathbf{r}+\mathbf{R})$ is periodic with respect to the lattice vector $\mathbf{R}$ generated by the primitive translation and it may be expanded in a Fourier series on $\mathbf{G}$, the reciprocal lattice vector:

$$\epsilon_{i,j}(\mathbf{r})=\sum_{\mathbf{G}}\epsilon_{i,j}(\mathbf{G})\exp(i\mathbf{G}\cdot\mathbf{r}) \quad (i,j=x,y). \tag{2}$$

A liquid crystal possesses two kinds of dielectric indices, that is, an ordinary dielectric index ϵ^0 and an extraordinary dielectric index ϵ^e. The light with the electric field perpen-

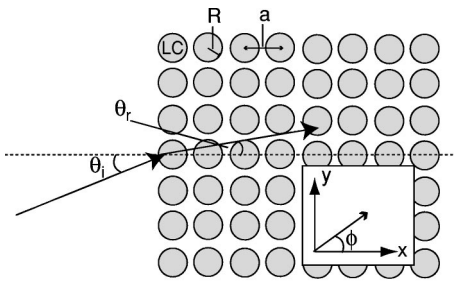

FIG. 1. Schematic model of light propagation from air regions to photonic crystals composed of liquid crystals. The arrow and ϕ in the diagram indicate the director and rotation angle of liquid crystals, respectively.

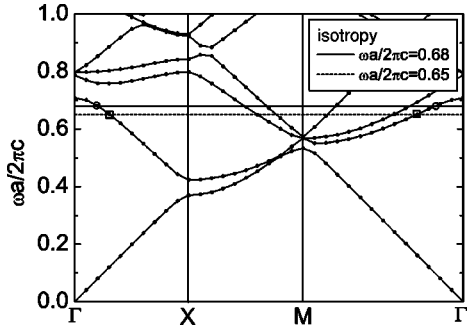

FIG. 2. Band structure of two-dimensional square-lattice photonic crystals when directors of liquid crystals are orientated at random. The circles and squares indicate intersection points of the second band at $\omega a/2\pi c=0.68$, and 0.65, respectively. The average refractive index of liquid crystals is $n_{LC}^{av}=1.583$.

dicular and parallel to the director of the liquid crystal feels ordinary and extraordinary refractive indices, respectively. In the case of directors of liquid crystals parallel to two-dimensional planes, the components of the dielectric tensor are represented as follows:

$$\epsilon_{x,x}(\mathbf{r})=\epsilon^{o}(\mathbf{r})\sin^2\phi+\epsilon^{e}(\mathbf{r})\cos^2\phi, \tag{3a}$$

$$\epsilon_{y,y}(\mathbf{r})=\epsilon^{o}(\mathbf{r})\cos^2\phi+\epsilon^{e}(\mathbf{r})\sin^2\phi, \tag{3b}$$

$$\epsilon_{x,y}(\mathbf{r})=\epsilon_{y,x}(\mathbf{r})=[\epsilon^{e}(\mathbf{r})-\epsilon^{o}(\mathbf{r})]\cos\phi\sin\phi, \tag{3c}$$

where ϕ is a rotation angle of the director of the liquid crystal and the director of liquid crystals is $\mathbf{n}=(\cos\phi,\sin\phi)$. In the isotropic case, $\epsilon^{o}(\mathbf{r})$ is equal to $\epsilon^{e}(\mathbf{r})$.

Equation (1) comprises a set of three coupled differential equations with periodic coefficients. In two-dimensional photonic crystals, we can define $\mathbf{e_G}$ as the direction perpendicular to the two-dimensional plane. Using Bloch's theorem, we may expand the magnetic field as

$$\mathbf{H}(\mathbf{r})=\sum_{\mathbf{G}} h(\mathbf{G})\mathbf{e_G}\exp\{i(\mathbf{k}+\mathbf{G})\cdot\mathbf{r}\} \tag{4}$$

in the case of the TE mode. Inserting Eqs. (2) and (4) into Eq. (1) and multiplying by $\mathbf{e_G}$ result in the following infinite matrix eigenvalue problem:

$$\sum_{\mathbf{G}'} H_{\mathbf{G},\mathbf{G}'}h(\mathbf{G}')=\frac{\omega^2}{c^2}h(\mathbf{G}), \tag{5a}$$

where

$$\begin{aligned}H_{\mathbf{G},\mathbf{G}'}=&\epsilon_{x,x}^{-1}(\mathbf{G}-\mathbf{G}')(k_y+G_y)(k_y+G_y')+\epsilon_{y,y}^{-1}(\mathbf{G}-\mathbf{G}')\\&\times(k_x+G_x)(k_x+G_x')-\epsilon_{x,y}^{-1}(\mathbf{G}-\mathbf{G}')(k_y+G_y)\\&\times(k_x+G_x')-\epsilon_{y,x}^{-1}(\mathbf{G}-\mathbf{G}')(k_x+G_x)(k_y+G_y').\end{aligned} \tag{5b}$$

For numerical purposes, Eq. (5a) is truncated by retaining only a finite number of reciprocal lattice vectors. The main numerical problem in obtaining the eigenvalue is the evaluation of the Fourier coefficients of the inverse dielectric tensors in Eq. (5b). The best method is to calculate the matrix of Fourier coefficients of real space constants and then take its inverse in order to obtain the required Fourier coefficients. This method was shown by Ho, Chan and Soukoulis (HCS) [15]. The eigenvalues computed with the HCS method for 289 plane waves are estimated to be in error less than 1%.

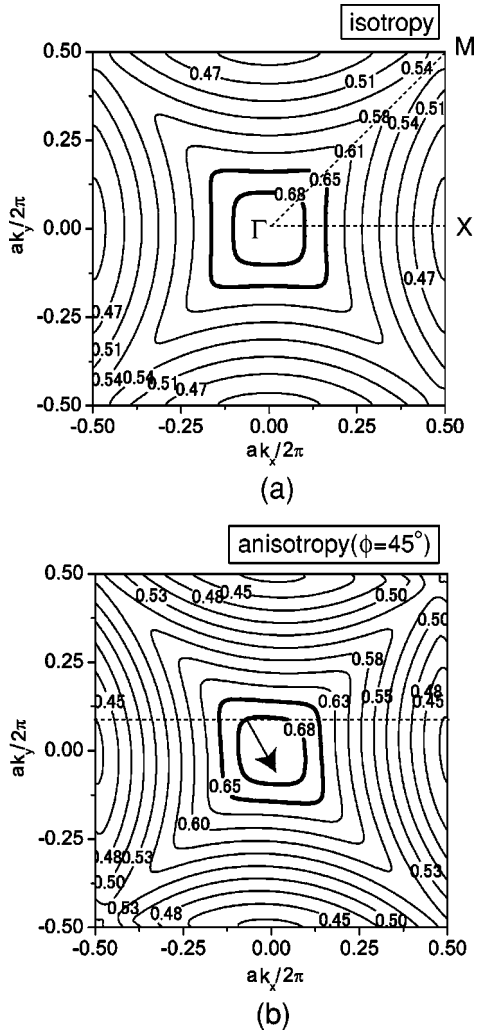

FIG. 3. Constant-frequency contours of the second band in the (a) isotropic and (b) anisotropic cases. In the isotropic case, directors of liquid crystals are orientated at random. In the anisotropic case, on the other hand, they are orientated at $\phi=45°$. Thick contours indicate the constant-frequency contours at $\omega a/2\pi c=0.68$, and 0.65. The ordinary and extraordinary refractive indices are $n_{LC}^{o}=1.522$ and $n_{LC}^{e}=1.706$, respectively.

Next, we investigate the light propagation in photonic crystals composed of liquid crystals. The velocity of light in photonic crystals is determined by the group velocity. The group velocity $\mathbf{v}_g$ satisfies the following equation:

$$\mathbf{v}_g=\frac{\partial\omega}{\partial\mathbf{k}}. \tag{6}$$

Using Hellmann and Feynman's theorem [19] we can obtain the following group velocity from Eq. (5a):

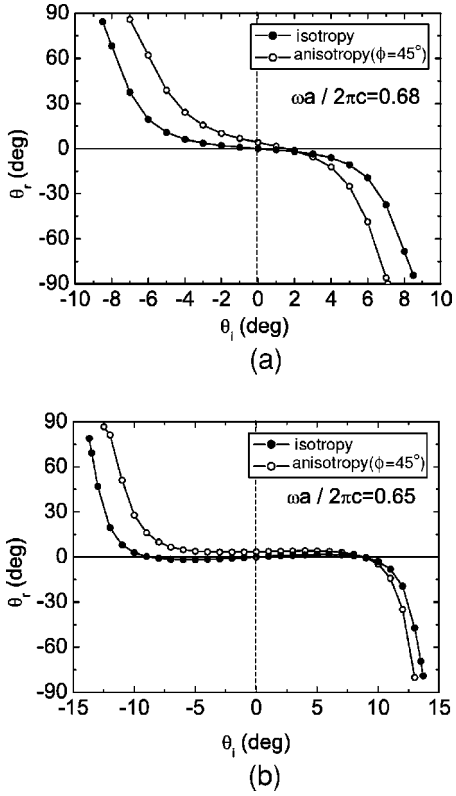

FIG. 4. Dependence of refractive angles on incident angles in the isotropic and anisotropic cases at $\omega a/2\pi c=$ (a) 0.68, (b) 0.65. In the isotropic case, directors of liquid crystals are orientated at random. In the anisotropic case, on the other hand, they are orientated at $\phi=45°$.

$$\mathbf{v}_g=\frac{\partial\omega}{\partial\mathbf{k}}=\frac{c^2}{2\omega}\sum_{\mathbf{G}}\sum_{\mathbf{G}'}h^*(\mathbf{G})\frac{\partial H_{\mathbf{G},\mathbf{G}'}}{\partial\mathbf{k}}h(\mathbf{G}'),\qquad(7a)$$

where

$$\sum_{\mathbf{G}}h^*(\mathbf{G})h(\mathbf{G})=1.\qquad(7b)$$

Therefore, the direction of the light propagation in photonic crystals is determined by Eq. (7a).

III. NUMERICAL CALCULATION AND DISCUSSION

Let us consider that the incident light propagates from air regions to photonic crystals, as shown in Fig. 1. We assume square-lattice photonic crystals composed of liquid-crystal rods, and that backgrounds are air regions. Such a condition could be realized by silica aerogels. Silica aerogels are porous structures and diameters of pores are about 20 nm. Refractive indices of silica aerogels are about 1.03, that is, they are almost the same as that of the air. Absorption of hydrophobic silica aerogels occurs around the infrared region [20]. Therefore, the hydrophobic silica aerogels are useful in the visible range. Indeed, hydrophobic silica aerogels are used as very low-refractive-index materials [21]. That is, the two-dimensional photonic crystals composed of liquid crystals can be prepared by making a periodic array of holes in the silica aerogel plate and then infiltrating liquid crystals into holes. When diameters of the holes are about 1 μm and are much larger than those of pores, wet liquid crystals can be trapped in the drilled holes. In making the holes in the silica aerogel plate by laser, moreover, pores around the holes may be broken by the heat of laser. Then, we do not have to consider leaking of liquid crystals into the pores around the holes. An experimental fabrication of tunable two-dimensional photonic crystals infiltrated with liquid crystals has already been reported [16].

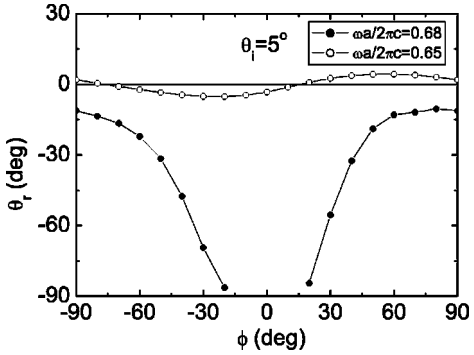

FIG. 5. Dependence of refractive angles on the rotation angle of liquid crystals ranging from $-90°$ to $90°$ at $\omega a/2\pi c=0.68$ and 0.65 when the incident angle is $5°$.

When we choose high-refractive-index materials as backgrounds, we cannot obtain high anisotropies caused by liquid crystals, although we can obtain high dispersion relations of frequencies and wave vectors. On the other hand, when we choose materials whose refractive indices are near those of liquid crystals as backgrounds, we cannot obtain high dispersion relations although we can obtain high anisotropies caused by liquid crystals. Therefore, we consider that the model we propose here is appropriate with respect to both high dispersion relations and high anisotropies.

We consider that ordinary and extraordinary refractive indices of liquid crystals are $n_{LC}^o=1.522$ and $n_{LC}^e=1.706$ (5CB), respectively, and that a radius of the rod is $R/a=0.4$. a is a lattice constant. In Fig. 1, θ_i and θ_r indicate incident and refractive angles, respectively, and ϕ in the diagram indicates the rotation angle of directors of liquid crystals.

When the electric field is not applied, directors of liquid crystals are orientated at random. That is, anisotropies of liquid crystals disappear and liquid crystals become isotropic, and then the average refractive index of liquid crystals is $n_{LC}^{av}=(n_{LC}^e+2n_{LC}^o)/3=1.583$.

In Fig. 2, we show the photonic band structure of photonic crystals composed of liquid crystals in the isotropic case. We consider two kinds of incident lights: one is the incident light at $\omega a/2\pi c=0.68$ and the other is the incident light at $\omega a/2\pi c=0.65$. The former is near the edge of the band gap and the latter is a little far from the edge of the band gap. We focus our attention on the second band in Fig. 2 although the third and forth bands also have wave vectors at $\omega a/2\pi c=0.68$, and 0.65. The circles and squares in Fig. 2 indicate intersection points of the second band at $\omega a/2\pi c=0.68$, and 0.65, respectively.

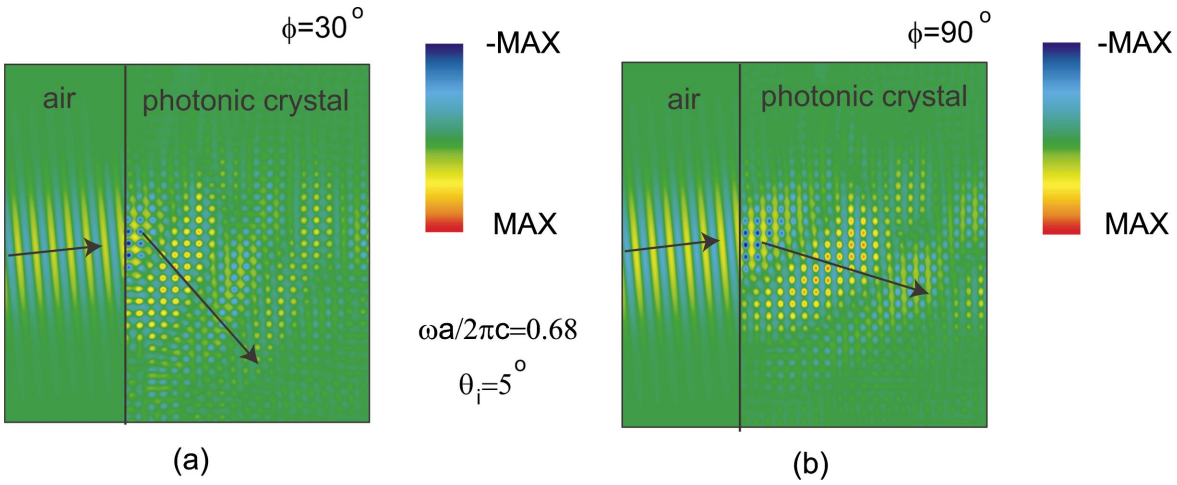

FIG. 6. (Color) Magnetic field patterns of light propagations at $\phi=$ (a) 30°, (b) 90° when the light at $\omega a/2\pi c=0.68$ is incident on photonic crystals at $\theta_i=5°$.

When the electric field is applied in two-dimensional planes, liquid crystals become anisotropic. Then, we cannot discuss by using the band structure in Fig. 2 because anisotropies of liquid crystals break the high rotational symmetry. In Fig. 3, we display the constant-frequency contours of the second band in the isotropic and anisotropic cases. Thick contours in Figs. 3(a) and 3(b) indicate the constant-frequency contours at $\omega a/2\pi c=0.68, 0.65$. Figure 3(a) shows the constant-frequency contours of the second band in Fig. 2 when the directors of liquid crystals are orientated at random, and Fig. 3(b) shows the constant-frequency contours of the second band when they are orientated at $\phi=45°$. As shown in Fig. 3(b), the high rotational symmetry in Fig. 3(a) disappears in the anisotropic case.

Next, we investigate refractive angles of the light propagating from air regions to photonic crystals composed of liquid crystals with anisotropies, as shown in Fig 1. By the momentum conservation in the y direction, the wave vector in the y direction in photonic crystals is given by

$$k_y=(2\pi/a)(\omega a/2\pi c)\sin\theta_i. \tag{8}$$

We can comprehend the schematic meaning of the light propagation in photonic crystals from Eq. (6). That is, this equation shows that the direction of the light propagation is equal to the normal direction to the constant-frequency contour. In Fig. 3(b), for example, a certain k_y of the light at $\omega a/2\pi c=0.68$ is shown as the broken line. We can calculate k_x and k_y by investigating intersection points between the break line and the constant-frequency contour at $\omega a/2\pi c=0.68$. The arrow in Fig. 3(b) indicates the direction of the light. However, we calculate refractive angles from Eq. (7a) in order to obtain high accuracies.

In Figs. 4(a) and 4(b), we display the dependence of refractive angles on incident angles in the isotropic and anisotropic ($\phi=45°$) cases at $\omega a/2\pi c=0.68$, and 0.65, respectively. Black and white points indicate isotropic and anisotropic cases, respectively. As shown in Fig. 4(a), signs of refractive angles are always opposite to those of incident angles regardless of the isotropic and anisotropic cases. That is, these conditions correspond to the negative refractive-index conditions. Changes of refractive indices in the anisotropic case is larger than those in the isotropic case.

As shown in Fig. 4(b), on the other hand, changes in refractive indices at $\omega a/2\pi c=0.65$ are not as large as those at $\omega a/2\pi c=0.68$, regardless of the isotropic and anisotropic cases. In the isotropic case, especially, relations between the incident and refractive angles in the range from about $-8°$ to about 8° satisfy $0<\theta_r<\theta_i$ in conventional-refractive-index materials, although negative refractions are shown in the range of incident angles from about $-14°$ to about $-10°$ and from about 10° to about 14°.

In the anisotropic case, however, it should be noted that θ_r is not equal to zero at $\theta_i=0$ due to anisotropies of liquid crystals in comparison with the isotropic case, as shown in Figs. 4(a) and 4(b). In Fig. 4(b), moreover, refractive angles are almost constant in the range of incident angles from about $-8°$ to about 8° in the anisotropic case. These are due to distortions of the constant-frequency contours caused by anisotropies of liquid crystals, as shown in Fig. 3(b). Therefore, anisotropies of liquid crystals provide peculiar negative refractions in comparison with the isotropic case.

In Fig. 5, we discuss the dependence of refractive angles on the rotation angles of liquid crystals ranging from $-90°$ to 90° at $\omega a/2\pi c=0.68$, and 0.65 when the incident angle is $\theta_i=5°$. Black and white points indicate $\omega a/2\pi c=0.68$, and 0.65, respectively. At $\omega a/2\pi c=0.68$, as shown in Fig. 5, refractive angles are sensitively affected by the change in rotation angles of liquid crystals, and are always negative. Moreover, there exist the rotation angles of liquid crystals at which light cannot be incident.

At $\omega a/2\pi c=0.65$, on the other hand, refractive angles do not change very largely although sings of refractive angles change from positive to negative. That is, refractive angles strongly depend on changing the rotation angles of liquid crystals as the frequency of the light becomes nearer the edge of the band gap.

In Fig. 6, we display the magnetic field pattern of the light propagation when the light at $\omega a/2\pi c=0.68$ is incident on

the photonic crystal at $\theta_i = 5°$ in order to investigate the tunable refraction effects in Fig. 5. Figures 6(a) and 6(b) show magnetic field patterns of light propagations at $\phi = 30°$, and 90°, respectively. The right half is a square photonic crystal with 31×21 unit cells. Arrows indicate directions of the light propagations. We used the finite difference time domain (FDTD) method in order to obtain the magnetic filed patterns of the light propagations. A more detailed treatment of the FDTD method is given in Ref. [22]. As shown in Fig. 6, the incident light propagates in photonic crystals efficiently, and the light beam does not mostly disperse in photonic crystals, which indicates that the photonic crystals we propose are efficient as optical devices.

In this figure, it should be noted that the direction of the light propagation is not normal to the wave front. This is because the group velocity is generally different from the phase velocity. The phase velocity is normal to the wave front, and the light propagation depends on the group velocity.

Figures 6(a) and 6(b) clearly show that the direction of light propagation can be changed by rotating the directors of liquid crystals, which indicates that we can obtain tunable refraction effects in two-dimensional photonic crystals utilizing liquid crystals.

IV. CONCLUSION

In conclusion, we theoretically demonstrated tunable refraction effects in two-dimensional photonic crystals utilizing liquid crystals. Due to liquid crystals with anisotropies, a high symmetry disappears in photonic crystals, and then the incident light propagates in photonic crystals at refractive angles different from those in photonic crystals composed of isotropic materials. Moreover, refractive angles can be changed by rotating directors of liquid crystals by applied voltages. Tunable refraction effects were also demonstrated for light with two kinds of frequencies: one is a frequency at the edge of bang gaps and the other is a frequency a little far from the edge of band gaps.

ACKNOWLEDGMENTS

This work was partly supported by a Grant-in-Aid for Scientific Research from the Ministry of Education, Culture, Sports, Science, and Technology (Grant No. 14205046) and from the Japan Society for the Promotion of Science, and by a NEDO International Joint Research Grant.

[1] E. Yablonovitch, Phys. Rev. Lett. **58**, 2059 (1987).
[2] S. John, Phys. Rev. Lett. **58**, 2486 (1987).
[3] S. John and T. Quang, Phys. Rev. Lett. **74**, 3419 (1995).
[4] S. John, Phys. Rev. Lett. **53**, 2169 (1984).
[5] A.Z. Genack and N. Garcia, Phys. Rev. Lett. **66**, 2064 (1991).
[6] D. Wiersma, P. Bartolini, A. Lagendijk, and R. Righini, Nature (London) **390**, 671 (1997).
[7] V.P. Bykov, Sov. J. Quantum Electron. **4**, 861 (1975).
[8] S. John and J. Wang, Phys. Rev. Lett. **64**, 2418 (1990).
[9] S. John and T. Quang, Phys. Rev. A **50**, 1764 (1994).
[10] T. Quang, M. Woldeyohannes, S. John, and G. S Agarwal, Phys. Rev. Lett. **79**, 5238 (1997).
[11] K. Yoshino, Y. Shimoda, Y. Kawagishi, K. Nakayama, and M. Ozaki, Appl. Phys. Lett. **75**, 932 (1999).
[12] Y. Shimoda, M. Ozaki, and K. Yoshino, Appl. Phys. Lett. **79**, 3627 (2001).
[13] M. Ozaki, Y. Shimoda, M. Kasano, and K. Yoshino, Adv. Mater. **14**, 514 (2002).
[14] K. Busch and S. John, Phys. Rev. Lett. **83**, 967 (1999).
[15] K. Busch and S. John, Phys. Rev. E **58**, 3896 (1998).
[16] S.W. Leonard, J.P. Mondia, H.M. van Driel, O. Toader, S. John, K. Busch, A. Birner, U. Gosele, and V. Lehmann, Phys. Rev. B **61**, R2389 (2000).
[17] S.Y. Lin, V.M. Hietala, L. Wang, and E.D. Jones, Opt. Lett. **21**, 1773 (1996).
[18] H. Kosaka, T. Kawashima, A. Tomita, M. Notomi, T. Tamamura, T. Sato, and S. Kawakami, Phys. Rev. B **58**, 10 096 (1998).
[19] For example, see Appendix B in K. Sakoda, and K. Ohtaka, Phys. Rev. B **54**, 5742 (1996).
[20] H. Yokogawa, J. Non-Cryst. Solids **186**, 23 (1995).
[21] T. Sumiyoshi, J. Non-Cryst. Solids **225**, 369 (1998).
[22] A. Taflove and S.C. Hagness, *Computational Electrodynamics: The Finite-Difference Time-Domain Method* (Artech House, Boston, 1995).